STATUS AND PERSPECTIVE OF EMITTER FORMATION BY POCl₃-DIFFUSION

A. Wolf, A. Kimmerle, S. Werner, S. Maier, U. Belledin, S. Meier, D. Biro
Fraunhofer Institute for Solar Energy Systems ISE, Heidenhofstraße 2, 79110 Freiburg, Germany
Telephone: +49 761 4588 5580, fax: +49 761 4588 7621, e-mail: andreas.wolf@ise.fraunhofer.de

ABSTRACT: The advances in contact formation of screen printed Ag pastes and the related progress in emitter profile tailoring has been a key driver for recent efficiency improvements. This paper summarizes the current status of phosphorus-diffused emitters for p-type silicon solar cells and discusses two technological options for advanced tube furnace POCl₃-diffusion processes: *diluted source* and *in-situ post oxidation*. Lower surface doping concentration levels are identified as key parameter for further reducing carrier recombination in the emitter. Using analytical modelling, we estimate potential efficiency improvements of 0.3%$_{abs}$ for PERC type solar cells from reducing the surface concentration from 2x10^{20} cm^{-3} down to 10^{19} cm^{-3}. We also address the increasing importance of recombination at the metal contacts and investigate the role of the diffusion profile and sheet resistance by analytical modelling. If metal contact recombination is supressed by a *selective emitter* and/or advanced *low recombination metallization pastes*, a potential efficiency gain of 0.5%$_{abs}$ is predicted.
Keywords: phosphorus-diffusion, emitter recombination, contact recombination, in-situ post oxidation,

1 INTRODUCTION

Tube furnace diffusion using phosphorus oxychloride (POCl₃) as dopant precursor is the dominating emitter formation technology for p-type Si solar cells [1, 2]. The reduction of emitter recombination, enabled by a fast progress of front contact paste development, has been a major driver for the efficiency improvements of the past years. In addition, the increasing market share of passivated emitter and rear (PERC)-type solar cells will draw more attention to the emitter properties, since recombination at the cell's rear surface is not limiting performance any more, as it is the case for Aluminium back surface field (Al-BSF) solar cells.

This work describes the properties of state of the art POCl₃-diffused emitters and discusses technological options for diffusion processes that omit the formation of recombination active defects related to inactive phosphorus doping. We also address possible limitations and industrial feasibility of these approaches. Assuming further progress for the development of metallization pastes, future emitters will feature phosphorus surface concentrations of a few 10^{19} cm^{-3}. Here, the question arises what levels of emitter recombination (passivated and metallized area) will be possible and which efficiency improvements can be expected. Analytical modelling based on a detailed experimental analysis quantifies the potential improvements for Al-BSF and PERC-type solar cells that are expected for a continued reduction of the surface doping levels. This includes an analysis of recombination at the metal contacts and a discussion on possible future technological trends.

2 STATUS OF POCl₃-DIFFUSION

The continuous progress in the development of Ag front metallization pastes has enabled the reduction of phosphorus near-surface doping levels while maintaining a sufficiently low specific contact resistance ρ_C [3, 4] . Current metallization pastes only require very little amount of non-active phosphorus to achieve low ohmic contact. This permits the use of diffusion processes with reduced amount of undissolved and electrically inactive phosphorus [5] and prevent the formation of Si-P precipitates [6] and other related defects, thereby reducing carrier recombination in the emitter.

2.1 Emitter properties

Figure 1 presents carrier concentration profiles for diffusion processes developed at Fraunhofer ISE [7] extracted from electrochemical capacity voltage (ECV) measurements on planar wafers. For process Gen1 (introduced at ISE in 2010) a high content of inactive phosphorus is expected, since the surface carrier concentration is close to solubility limit of phosphorus in silicon [8]. For diffusion processes of this type, phosphorus concentrations exceeding the solubility limit are confirmed by secondary ion mass spectroscopy (not shown here). Continuous development of the diffusion process resulted in doping profiles of Gen2 and Gen3 with lower surface carrier concentration. Gen3 (introduced at ISE in 2014) exhibits a surface carrier concentration well below the phosphorus-solubility and thus only a marginal content of supersaturated phosphorus is expected.
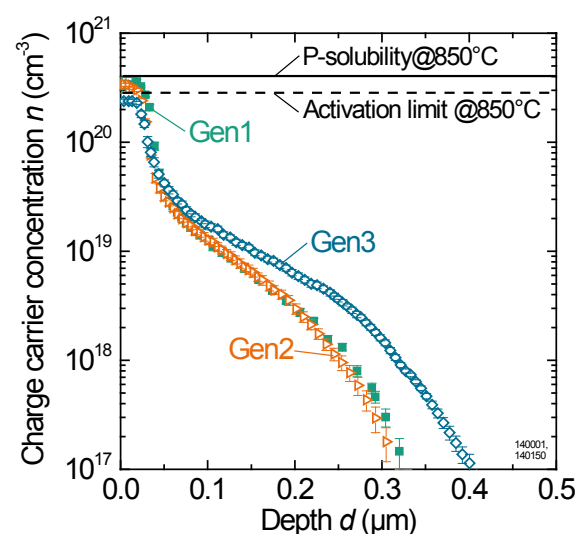

Figure 1: Carrier concentration profiles resulting from different diffusion processes measured by ECV on planar wafers. For comparison, the P-solubility limit and the dopant activation limit from Ref [8] are stated.
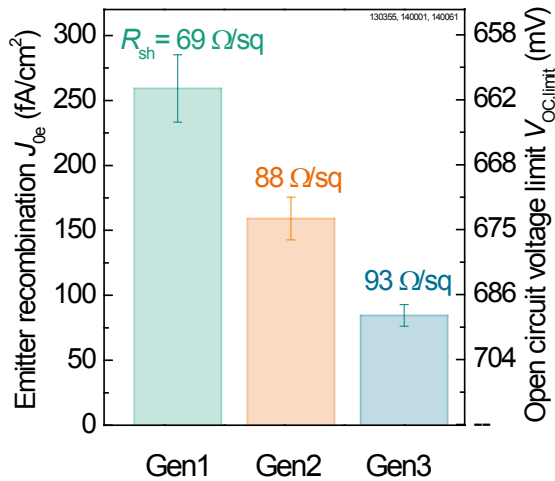
Figure 2: Recombination parameter J_{0e} (left scale, avg. value and std. dev. of 5 measurement points per wafer) and associated voltage limit $V_{OC,limit}$ (right scale, for 25°C and J_{SC} = 39 mA/cm²) determined for symmetric alkaline textured, PECVD SiN_X-passivated samples after contact firing. The corresponding sheet resistance R_{sh} is given for textured surface after PSG removal

We process both sides alkaline textured and diffused samples using Czochralski (Cz)-grown n-type Si wafers with a resistivity of 5.7 Ωcm (determined after thermal process). After SiN_X-passivation and simulated contact firing we extract the recombination parameter J_{0e} from quasi steady state photo conductance (QSSPC) measurements using the method described in Ref. [9]. Figure 2 shows J_{0e} and the associated open circuit voltage limit $V_{OC,limit}$ for the three diffusion processes. Apparently, the doping profile tailoring to reduce the surface doping concentration from Gen1 to Gen3 has decreased carrier recombination by a factor of three pushing up the V_{OC}-limitation by more than 30 mV. Screen printed silver contacts using commercial, state of the art metallization pastes yield low ohmic contacts with ρ_C < 5 mΩcm² for emitter Gen3 [7]

In conclusion, the present emitters are virtually free of undissolved phosphorus dopants and therefore allow for recombination parameters J_{0e} well below 100 fA/cm². Thus, surface and Auger recombination are the two remaining dominant contributions to J_{0e}. Despite the absence of supersaturated phosphorus, recent emitters provide sufficiently low contact resistance for current screen printed metallization pastes.

2.2 Diffusion process
There are two frequently applied strategies for reducing the surface concentration of phosphorus which thereby minimize or avoid the generation of undissolved and inactive dopants and related defects during diffusion. A widespread strategy is the use of a *diluted source*, meaning a reduction of the phosphorus concentration in the phosphosilicate glass (PSG) layer. This is achieved by e.g. decreasing the ratio of POCl₃ to oxygen in the process atmosphere during the PSG growth at the beginning of the diffusion process [5]. Currently, such PSG deposition processes apply oxygen gas flows several times higher than the nitrogen gas flow through the POCl₃ bubbler [10]. While this approach has been successfully used to reduce emitter recombination [5], it

inherently increases the non-uniformity of the PSG layer for processes that aim at low surface concentration levels. Since phosphorous containing atmosphere reacts with the wafer surface to form the PSG layer, the local phosphorous concentration at the centre of the wafer reduces compared to the edges, yielding a reduced local PSG thickness and different composition. It is thus a challenge to maintain an acceptable uniformity of the sheet resistance across the wafer surface and the full load process boat at a reasonable time span for the PSG growth. The use of low pressure diffusion processes [11] facilitates the realization of acceptable uniformity with a *diluted source*, although placing the wafers at half pitch for increased throughput again partly sacrifices this advantage.

The second approach applies *in-situ post oxidation* [12, 13]. Here, a moderate ratio of POCl₃ to oxygen is chosen for the process atmosphere during PSG growth followed by a process phase with high oxygen concentration, preferably at increased temperatures. During this second process phase an intermediate thermal oxide layer grows at the Si surface and decouples the PSG layer from the Si wafer, which retards the prolonged in-diffusion of phosphorus. In parallel, the highly doped silicon surface is transformed into SiO_2, which is subsequently removed in the PSG etch process. This allows for higher POCl₃ concentration during PSG growth and is thus less challenging regarding uniformity of the sheet resistance. However, a strong post oxidation requires a higher temperature compared to the process phase for PSG growth and thus a second temperature plateau, which increases process time and costs. Processes applied in production currently often use a combination of both approaches *diluted source* and *in-situ post oxidation*.
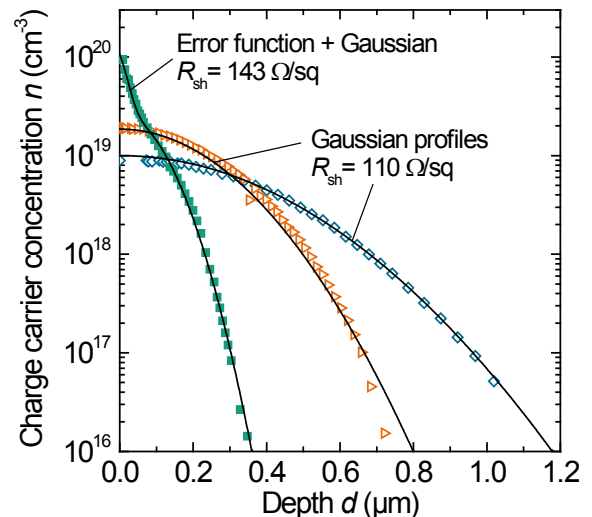

Figure 3: Carrier concentration profiles (symbols) resulting from different *in-situ post oxidation* diffusion processes, measured by ECV on planar wafers. The lines represent fits using either a sum of an error function and a Gaussian curve or a sole Gaussian profile.

3 PERSPECTIVE AND POTENTIAL

Results at Fraunhofer ISE show that *in-situ post oxidation* is suited to reduce the surface doping concentration n_{surf} to levels as low as 1×10^{19} cm^{-3}. Figure 3 shows doping profiles achieved in one single thermal process by means of *in-situ post oxidation*. Apparently, various surface concentrations and profile depth are feasible and both parameters can be adjusted independently to a certain extend. Processes that apply a strong *in-situ post oxidation* yield Gaussian-shaped profiles. Such diffusion processes still show sufficient uniformity of 5 to 6% (standard deviation over wafer surface). In contrast, it seems very challenging to achieve surface concentrations in the range of a few 10^{19} cm^{-3} and maintain sufficient uniformity over wafer and process boat with a sole *diluted source* approach. However, profiles with low surface concentrations may also be obtained by conventional strong diffusion processes with extended temperature and time and subsequent back etching of the highly doped surface layer in a second process step [14]. Similarly, challenges for a strong *in-situ post oxidation* are long process times as well due to extended drive in time (120 min for the profile with $n_{surf} \approx 2\times10^{19}$ cm^{-3} from Figure 3) and possible negative impacts on the Si wafer [15, 16]. These issues need to be addressed to exploit the potential of reduced emitter recombination.

3.1 Emitter recombination

We apply analytical models [17, 18] to determine the potential for continued reduction of carrier recombination in the emitter by reducing surface doping levels even further. Recent experiments at Fraunhofer ISE [19] yield surface recombination velocity (SRV) of phosphorus doped, alkaline textured surfaces for different surface doping concentration levels n_{surf}. Investigated passivation schemes are plasma enhanced chemical vapour deposited (PECVD) SiO$_X$N$_Y$/SiN$_X$ [20] and thermal SiO$_2$/PECVD SiN$_X$ stacks, both activated by a conventional contact firing process. Both approaches show quite similar passivation quality, superior to single (non-graded) SiN$_X$ layers. In this work a PECVD-based passivation by SiO$_X$N$_Y$/SiN$_X$ is assumed with a SRV of 17000 cm/s for $n_{surf} = 2\times10^{20}$ cm^{-3} and 2200 cm/s for $n_{surf} = 1\times10^{19}$ cm^{-3} [19].

The ITRPV roadmap predicts a moderate increase in sheet resistance from present $R_{sh} = 100$ Ω/sq to 110 Ω/sq in 2018 and 120 Ω/sq in 2021 [21]. We therefore generate artificial doping profiles with varying n_{surf} but constant $R_{sh} = 110$ Ω/sq, as depicted in Figure 4 (lines). The sum of an error function (kink) and a Gaussian function (tail) for $n_{surf} > 5\times10^{19}$ cm^{-3} or a sole Gaussian curve for $n_{surf} < 5\times10^{19}$ cm^{-3} yields good accordance with some experimental profiles (see Figure 3).

We calculate J_{0e} of the textured and passivated front surface for the doping profiles shown in Figure 4 using models and parameters from Ref. [19]. The model accounts for the textured surface by multiplying the result for planar surface with a factor of 1.6., as observed in measurements and applied for the determination of the SRV [19]. As a result, reducing n_{surf} from 2×10^{20} cm^{-3} to 10^{19} cm^{-3} will reduce the recombination in the passivated area from above 100 fA/cm² to below 40 fA/cm², although the sheet resistance is maintained at $R_{sh} = 110$ Ω/sq.

3.2 Metal contact recombination

Current front Ag pastes exhibit a recombination at the metal contacts of $J_{0,met} < 1000$ fA/cm² at surface doping levels of 2 to 3×10^{20} cm^{-3} and a sheet resistance of 80 to 110 Ω/sq [22]. These values are reproduced by the analytical model assuming a penetration depth of 25 nm for the metal contact, realized by a SRV of $S_p = 3\times10^6$ cm/s at a profile depth of $d_{met} = 25$ nm. Figure 5 presents the calculated $J_{0,met}$ dependence on the surface concentration for $R_{sh} = 90$ and 110 Ω/sq (profiles see Figure 4). The applied parameters lead to a metal recombination that is quite independent on the surface concentration, especially for $n_{surf} < 10^{20}$ cm^{-3}. Apparently,

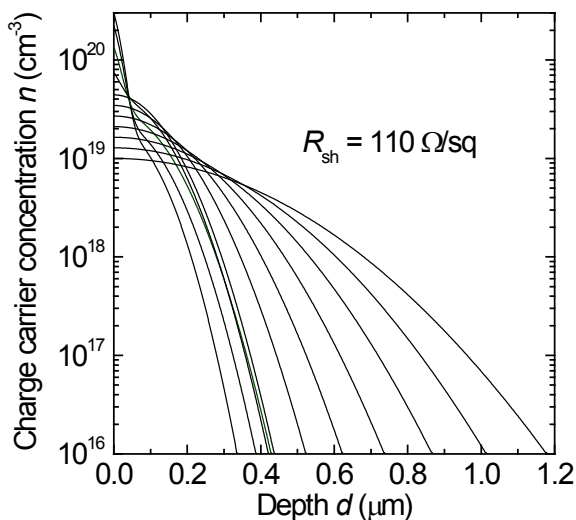
Figure 4: Artificial diffusion profiles for different n_{surf} at constant $R_{sh} = 110$ Ω/sq generated using either the sum of an error function and a Gaussian function for $n_{surf} > 5\times10^{19}$ cm^{-3} or a sole Gaussian curve for $n_{surf} < 5\times10^{19}$ cm^{-3} This setup reproduces experimental profiles quite well (see Figure 3)
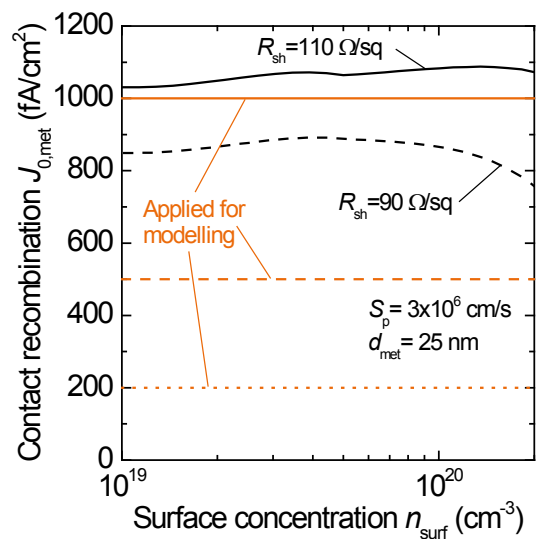

Figure 5: Analytically calculated surface concentration dependence of the contact recombination $J_{0,met}$ (curves) for two R_{sh}-values. The applied carrier profiles for $R_{sh} = 110$ Ω/sq are depicted in Figure 4. The horizontal lines represent constant $J_{0,met}$-values used for modelling the cell performance.
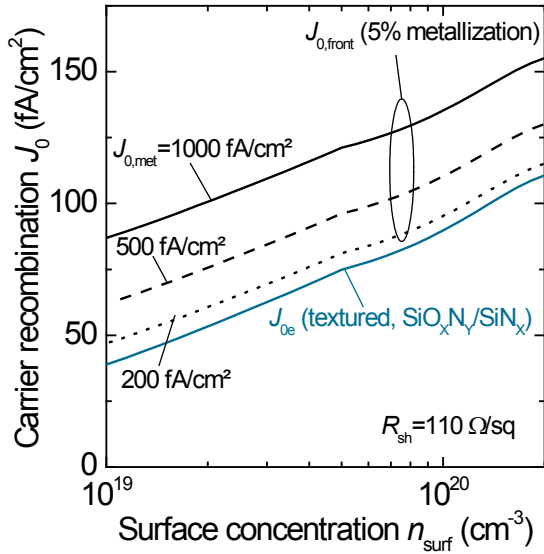
Figure 6: Analytically calculated recombination parameter as a function of surface carrier concentration for a constant sheet resistance of 110 Ω/sq (profiles see Figure 4). Stated are J_{0e} for the textured and PECVD SiO_XN_Y/SiN_X-passivated area and the total recombination $J_{0,front}$ from Eq. (1) including 5% metallization for three different constant $J_{0,met}$-values.

it is rather the total doping dose (thus sheet resistance) that affects $J_{0,met}$, the profile shape seems to have smaller impact. We therefore apply three different $J_{0,met}$-values and assume that $J_{0,met}$ does not depend on the surface concentration (horizontal lines in Figure 5). Here, $J_{0,met} = 1000$ fA/cm² represents current metallization pastes. Future paste development should lead to reduced contact recombination, thus $J_{0,met} = 500$ fA/cm² simulates a *low recombination paste* scenario. Contact recombination is further suppressed by paste development and/or the implementation of a selective emitter [14, 23], represented by $J_{0,met} = 200$ fA/cm². This *selective emitter* scenario assumes perfect alignment.

Figure 6 presents the resulting total front recombination

$$J_{0,front} = 0.95 \cdot J_{0e} + 0.05 \cdot J_{0,met} \qquad (1)$$

for the three scenarios assuming 5% metal coverage. For current metallization pastes, the reduction of n_{surf} from 2×10^{20} cm⁻³ to 10^{19} cm⁻³ will lead to a 44% lower total front recombination of $J_{0,front} = 87$ fA/cm². In parallel, the contribution of the contact recombination rises from 28% to 55%. In the *low recombination paste* scenario, at $n_{surf} = 10^{19}$ cm⁻³ still 40% of $J_{0,front}$ originates from contact recombination which further reduces to 21% in the *selective emitter* scenario. For the latter, the total front recombination is suppressed to below 50 fA/cm².

3.3 Solar cell performance

We calculate expected improvements for monocrystalline Al-BSF and PERC-type solar cells enabled by lower n_{surf} and thus reduced $J_{0,front}$ using a two diode model. Table I lists the input parameters with the short circuit current density for perfect blue response J_{SC0}, the base recombination J_{0b}, the second diode recombination J_{02}, and the lumped series resistance R_S.

Table I: Input parameters for the two diode model for the considered solar cell types

Parameter	Al BSF	PERC
J_{SC0} (mA/cm²)	38	39
J_{0b} (fA(/cm²)	400	100
J_{02} (nA/cm²)	3	3
R_S (Ωcm²)	0.6	0.7

The previously discussed analytical model yields the total front recombination $J_{0,front}$ from Eq. (1) and the loss in short circuit current ΔJ_{SC} due to emitter recombination. The two diode model then applies $J_{01} = J_{0,front} + J_{0b}$ and $J_{SC} = J_{SC0} - \Delta J_{SC}$. It is assumed that future metallization paste generations will maintain current contact resistance levels although n_{surf} is reduced, leading to a constant R_S.

Figure 6 shows expected improvements for the open circuit voltage V_{OC} and efficiency η of Al-BSF and PERC-type solar cells enabled by lower surface concentration and thus reduced emitter recombination. For the scenario with $J_{0,met} = 1000$ fA/cm², a gain of 8 mV in V_{OC} and 0.3%$_{abs}$ in efficiency is predicted for

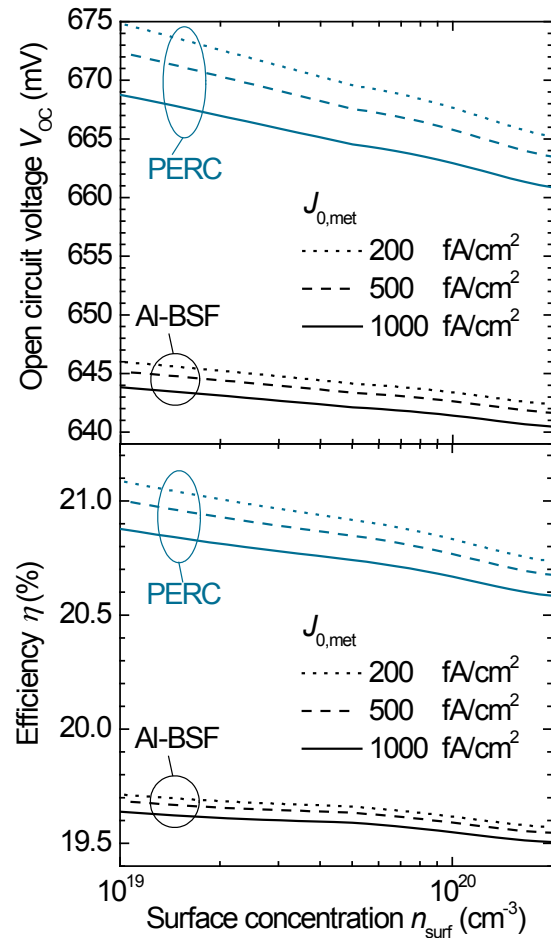
Figure 7: Open circuit voltage (top) and efficiency (bottom) vs. emitter surface concentration (constant $R_{sh} = 110$ Ω/sq) for Al-BSF and PERC type solar cells resulting from the two diode model (Table I) for the three described scenarios with different constant metal recombination parameters $J_{0,met}$.

PERC type solar cells when reducing n_{surf} from 2×10^{20} cm^{-3} down to 10^{19} cm^{-3}. If simultaneously contact recombination is reduced to $J_{0,met} = 500$ or 200 fA/cm² by e.g. paste improvements or a (perfectly aligned) selective emitter, a V_{OC}-increase of 12 and 14 mV, respectively, can be expected. The corresponding efficiency gain is 0.4 and 0.5 %$_{abs}$, respectively. In the case of Al-BSF type solar cells only slight improvements are expected when reducing the surface concentration in all three scenarios, since high base recombination limits the performance for this cell type.

4   SUMMARY AND CONCLUSION

Current front metallization pastes yield specific contact resistances of $\rho_C < 5$ mΩcm² for surface doping levels that are essentially free of supersaturated phosphorus and related defects, leaving surface and Auger recombination as the major recombination mechanisms. Such emitters exhibit recombination current densities J_{0e} below 100 fA/cm² (textured, passivated area) at a sheet resistance of 80 to 100 Ω/sq . The technological approaches for present and future POCl$_3$ diffusion process development include lowly concentrated phosphosilicate glass layers (*diluted source*) as well as *in-situ post oxidation*. While both routes will require increased process times for formation of advanced emitters, the *diluted source* option faces inherent challenges for sheet resistance uniformity and limitations for achievable lower limits of near-surface doping concentration. By contrast, doping levels of 10^{19} cm^{-3} and lower are feasible with *in-situ post oxidation* while maintaining a sufficient sheet resistance uniformity over the wafer surface and the process boat. Although present metallization pastes show increased tolerance to sheet resistance non-uniformity, we expect that future diffusion processes will tend to apply *in-situ post oxidation* to further reduce surface concentration levels, facing challenges of extended process times and possible negative impacts on the Si wafer.

We apply an analytical model to calculate carrier recombination in the emitter for doping profiles with surface concentrations between $n_{surf} = 2\times10^{20}$ cm^{-3} and 10^{19} cm^{-3} at a constant sheet resistance of 110 Ω/sq. A reduction of n_{surf} to 10^{19} cm^{-3} will reduce J_{0e} below 40 fA/cm² (textured, PECVD-passivated). An analysis of the recombination underneath the metal contacts predicts that for a fixed sheet resistance, a change in surface concentration for values $n_{surf} < 10^{20}$ cm^{-3} will have a minor impact on contact recombination. It is thus rather the doping dose (sheet resistance) than the profile shape that affects contact recombination.

Assuming that future metallization pastes will maintain current contact resistance and contact recombination values, a reduction of n_{surf} from 2×10^{20} cm^{-3} to 10^{19} cm^{-3} will enable 8 mV and 0.3%$_{abs}$ gain in V_{OC} and efficiency, respectively, for PERC type solar cells. If in parallel to the n_{surf} reduction, contact recombination is supressed from presently $J_{0,met} = 1000$ to 200 fA/cm², our simulations predict potential improvements of up to 14 mV in V_{OC} and 0.5%$_{abs}$ in efficiency

In conclusion, the reduction of the surface concentration by e.g. *in-situ post oxidation* or back etching after the diffusion process is the key parameter for further suppressing emitter recombination. We expect

that the increasing importance of contact recombination at reduced surface concentration levels will retard or even reverse the trend to higher sheet resistances in the case of homogeneous emitters. This development will also drive technological efforts to reduce contact recombination losses by either novel *low recombination pastes* and / or the re-introduction of *selective emitters* or alternative metallization approaches.

REFERENCES

[1]   S. Peters, "Industrial diffusion of phosphorous n-type emitters for standard wafer-based silicon solar cells," *Photovoltaics International*, no. 3, pp. 60–66, 2009.

[2]   A. Bentzen, "Phosphorus diffusion and gettering in silicon solar cells," Dissertation, Department of Physics, Oslo, University of, Oslo.

[3]   M. Z. Burrows, A. Meisel, D. Balakrishnan, A. Tran, D. Inns, L. Dellis, E. Kim, A. F. Carroll, and K. R. Mikeska, "Front-Side Silver Contacts with Improved Recombination and Fine-Line Performance," in *28th EUPVSEC Paris: 2013*, 2013, pp. 1985–1988.

[4]   V. Shanmugam, J. Cunnusamy, A. Khanna, P. K. Basu, Y. Zhang, C. Chen, A. F. Stassen, M. B. Boreland, T. Mueller, B. Hoex, and A. G. Aberle, "Electrical and Microstructural Analysis of Contact Formation on Lightly Doped Phosphorus Emitters Using Thick-Film Ag Screen Printing Pastes," *IEEE J. Photovoltaics*, vol. 4, no. 1, pp. 168–174, 2014.

[5]   A. Dastgheib-Shirazi, M. Steyer, G. Micard, H. Wagner, P. P. Altermatt, and G. Hahn, "Relationships between Diffusion Parameters and Phosphorus Precipitation during the POCl3 Diffusion Process," *Energy Procedia*, vol. 38, pp. 254–262, 2013.

[6]   J. Horzel, B. Schum, A. Lachowicz, J. Rossa, K. Vaas, M. Jahn, Y. Gassenbauer, H. von Campe, H. Boubekeur, G. Blendin, U. Weber, A. Seidl, A. Armigliato, F. Seidel, T. Hantschel, P. Eyben, S. Vinzelberg, Gerstl, S. S. A, and W. Schmidt, "On anomalous emitter regions forming during phosphorous diffusion processing of crystalline silicon solar cells," in *25th EUPVSEC Valencia: 2010*, 2010, pp. 1882–1891.

[7]   S. Werner, E. Lohmüller, S. Maier, A. Kimmerle, A. Spribille, S. Wasmer, F. Clement, and A. Wolf, "Process optimization for the front side of p-type silicon solar cells," in *29th EUPVSEC Amsterdam: 2014*, 2014, pp. 1342–1347.

[8]   S. Solmi, A. Parisini, R. Angelucci, A. Armigliato, D. Nobili, and L. Moro, "Dopant and carrier concentration in Si in equilibrium with monoclinic SiP precipitates," *Phys. Rev. B*, vol. 53, no. 12, pp. 7836–7841, 1996.

[9]   A. L. Blum, J. S. Swirhun, R. A. Sinton, and A. Kimmerle, "An updated analysis to the WCT-120 QSSPC measurement system using advanced device physics," in *28th EUPVSEC Paris: 2013*, 2013, pp. 1521–1523.

[10]   N. Wehmeier, G. Schraps, H. Wagner, B. Lim, N. P. Harder, and P. P. Altermatt, "Boron-Doped PECVD Silicon Oxides as Diffusion Sources for Simplified High-Efficiency Solar Cell Fabrication," in *28th EUPVSEC Paris: 2013*, 2013, pp. 1980–1984.

[11]   M. Muehlbauer, A. Piechulla, C. Voyer, M. Citro, R. Dahl, and P. Fath, "Industrial Low-Pressure Phosphorus Diffusion for High Performance and Excellent Uniformity," in *26th EUPVSEC Hamburg: 2011*, 2011, pp. 2028–2030.

[12]   A. Cuevas, "A good recipe to make silicon solar cells," in *22nd IEEE Photovoltaic Specialists Conference Las Vegas: 1991*, 1991, pp. 466–470.

[13]   A. Kimmerle, R. Woehl, A. Wolf, and D. Biro, "Simplified Front Surface Field Formation for Back Contacted Silicon Solar Cells," *Energy Procedia*, vol. 38, no. 0, pp. 278–282, 2013.

[14]   G. Hahn, "Status of selective emitter technology," in *25th EUPVSEC Valencia: 2010*, 2010, pp. 1091–1096.

[15]   J. Haunschild, J. Broisch, I. Reis, and S. Rein, "Cz-Si wafers in solar cell production: Efficiency-limiting defects and material quality control," *Photovoltaics International*, no. 15, pp. 40–46, 2012.

[16]   A. Bentzen and A. Holt, "Overview of phosphorus diffusion and gettering in multicrystalline silicon," *Mat Sci Eng B-Solid*, vol. 159-160, pp. 228–234, 2009.

[17]   A. Cuevas, R. Merchan, and J. C. Ramos, "On the systematic analytical solutions for minority-carrier transport in nonuniform doped semiconductors: application to solar cells," *IEEE Trans. Electron Devices*, vol. 40, no. 6, pp. 1181–1183, 1993.

[18]   A. Kimmerle, A. Wolf, U. Belledin, and D. Biro, "Modelling carrier recombination in highly phosphorus-doped industrial emitters," *Energy Procedia*, vol. 8, pp. 275–281, 2011.

[19]   A. Kimmerle, R. Momtazur, S. Werner, S. Mack, A. Wolf, A. Richter, and H. Haug, *J. Appl. Phys,* submitted.

[20]   J. Seiffe, L. Weiss, M. Hofmann, L. Gautero, and J. Rentsch, "Alternative rear surface passivation for industrial cell production," in *23rd EUPVSEC Valencia: 2008*, 2008, pp. 1700–1703.

[21]   International Technology Roadmap for Photovoltaic, *2013 Results.*

[22]   T. Fellmeth, "Silicon Solar Cells for the Application in Low Concentrator Systems-Development and Characterization," Dissertation, 2014.

[23]   U. Jäger, S. Mack, C. Wufka, A. Wolf, D. Biro, and R. Preu, "Benefit of selective emitters for p-Type silicon solar cells with passivated surfaces," *IEEE J. Photovoltaics*, vol. 3, no. 2, pp. 621–627, 2013.